

World Applied Sciences Journal 18 (12): 1727-1736, 2012

ISSN 1818-4952

© IDOSI Publications, 2012

DOI: 10.5829/idosi.wasj.2012.18.12.2484

## Optimization of Baffle Spacing on Heat Transfer, Pressure Drop and Estimated Price in a Shell-and-Tube Heat Exchanger

<sup>1</sup>Ali Falavand Jozaei, <sup>2</sup>Alireza Baheri, <sup>3</sup>Mariam K. Hafshejani and <sup>4</sup>Armin Arad

<sup>1</sup>Department of Engineering, Ahvaz Branch, Islamic Azad University, Ahvaz, Iran

<sup>2</sup>Department of Engineering, Dezful Branch, Islamic Azad University, Dezful, Iran

<sup>3</sup>Shahrekord University of Medical Sciences, Shahrekord, Iran

<sup>4</sup>North Khorasan University of Medical Sciences, Bojnurd, Iran

---

**Abstract:** In this paper for a given heat duty, study of the effects of baffle spacing on three parameters mentioned above is considered in a STHX with single segmental baffles and staggered tubes layout in Iran, Arvand petrochemical. A program in EES (Engineering Equations Solver) software is used for this purpose to solve governing equations; moreover, Aspen BJAC and HTFS<sup>+</sup> softwares are used for considering estimated total price. At first the simulated results obtained from this program is compared to the experimental data for two cases of baffle spacing. The effects of baffle spacing are considered from 4 to 24 inches over overall heat transfer coefficient (OHTC) to pressure drop ratio ( $U/\Delta p$  ratio). The results show that  $U/\Delta p$  ratio is low when baffle spacing is minimum (4 inches) because pressure drop is high; however, heat transfer coefficient is very significant. And in this case estimated total price increases 7 percent. Then with the increase of baffle spacing, pressure drop rapidly decreases and OHTC also decreases, but the decrease of OHTC is lower than pressure drop, so ( $U/\Delta p$ ) ratio increases. After increasing baffles more than 12 inches, variation in pressure drop is gradual and approximately constant and OHTC decreases; Consequently,  $U/\Delta p$  ratio decreases again. If baffle spacing reaches to 24 inches, STHX will have minimum pressure drop, but OHTC decreases, so required heat transfer surface increases and  $U/\Delta p$  ratio decreases. After baffle spacing more than 12 inches, variation of both estimated price and shell side pressure drop is negligible. So optimum baffle spacing is suggested between 8 to 12 inches (43 to 63 percent of inside shell diameter) for a sufficient heat duty, low cost and low pressure drop.

**Key words:** Shell and tube heat exchanger . single segmental baffle . overall heat transfer coefficient . pressure drop

---

### INTRODUCTION

Although today a set of common types of heat exchangers (such as: double-pipe, spiral, plate and frame, plate-fin, compact heat exchangers) are used in heat transfer applications, the shell and tube heat exchangers (STHXs) are still the most common type in use. The STHX provides a comparatively large ratio of heat transfer area to volume and weight. STHXs are widely used in many industrial areas such as chemical process, power generation, petroleum refining, refrigeration, air-conditioning and etc [1-12]. The main objective in any heat exchanger design is the estimation of the minimum heat transfer area required for a given heat duty, as it governs the overall cost of the heat exchanger. The baffles are of primary importance in improving mixing levels and consequently enhancing heat transfer of STHXs. Segmental baffles are most commonly used in STHXs. The most-commonly used baffle is the segmental baffle, which forces the shell side fluid going through in a zigzag manner, hence, improves the heat transfer with a large pressure drop penalty. Baffles are provided for heat transfer purposes and are used to support tubes, enable a desirable velocity to be maintained for the shell side fluid and prevent vibration of the tubes.

Study of baffle spacing in STHXs for optimization of heat transfer, pressure drop and estimate total price is less considered numerical and experimental simultaneously. One of the effective factors on parameters mentioned above is baffle spacing and the paper written by Huadong and Volker [13] considers only local heat transfer coefficient distribution at an individual tube and the percentage of the leakage stream due to the higher flow velocity through

---

**Corresponding Author:** Ali Falavand Jozaei, Department of Engineering, Ahvaz Branch, Islamic Azad University, Ahvaz, Iran

Table 1: Geometric parameters

Dimension	Value
Heat Exchanger Type (TEMA)	BEM
Shell inside Diameter (mm)	477.8
No. shell passes	1
No. Tube passes	1
Tube OD× wall thk.(mm)	25.4×2
No. of Tubes	160
Tube layout (pattern)	Triangular, 30°
Tube pitch (mm)	31.8
Tube Length (mm)	4270
Baffles type baffles cut pct of dia./orientation	Single Segmental22%
No. of initial baffles	16

Table 2: Thermophysical properties

Fluid allocation	Shell side		Tube side	
	Cooling water		Low boils	
Fluid name	-----		-----	
	Inlet	Outlet	Inlet	Outlet
Mass flow (kg/h)	26172	26172	46998 (Liquid)+910 (Vapor)	47908 (Liquid)
Operating temperature (°C)	35	45	65	50
Density (kg/m <sup>3</sup> )	994.28	990.45	1273.013	1296.615
Specific heat (kJ/kg.K)	4.178	4.178	1.232	1.194
Thermal conductivity (W/m.K)	0.623	0.635	0.111	0.115
Fouling factor	0.00034 m <sup>2</sup> .k/w		0.0002 m <sup>2</sup> .k/w	

the baffle opening. But variation of baffle spacing is not considered on U/Δp ratio and estimated total price. So in this paper, this matter is considered numerical and experimental simultaneously. Also In this paper, the effects of baffle spacing are considered for the STHX (42E-13014) with geometric parameters and thermo-physical properties (Table 1 and 2) in Iran, Arvand Petrochemical.

### CALCULATION OF SHELL SIDE HEAT TRANSFER

The shell-side fluid flow model by Tinker proposed shown in Fig. 1. He also provided a method for determination of the individual flow stream components from which the overall heat transfer coefficient and pressure loss could be determined.

Although the Tinker method was later simplified by Fraas [14]. A correction factor was later applied to heat transfer coefficients obtained from these methods to account for all the leakage streams.

Bell-Delaware method accounts for the various leakage streams and involves relatively straightforward calculations. In the Bell-Delaware method, an ideal heat transfer coefficient  $h_{id}$  is determined for pure cross flow using the entire shell-side fluid flow stream at (or near) the center of the shell. It is computed from the correlations of Zhukauskas for staggered tube bundles with the number of tube rows  $n_r \geq 16$  [15].

$$Nu_d = \begin{cases} 1.04R_{ed}^{0.4}Pr^{0.36}Y^{0.25} & \text{for } 1 \leq R_{ed} < 500 \\ 0.71R_{ed}^{0.5}Pr^{0.36}Y^{0.25} & \text{for } 500 \leq R_{ed} < 1000 \\ 0.35\varrho^{0.2}R_{ed}^{0.63}Pr^{0.36}Y^{0.25} & \text{for } 1000 \leq R_{ed} < 2 \times 10^5 \end{cases} \quad (1)$$

Where:  $Y = \frac{Pr}{Pr_w}$  and  $\varrho = \frac{X_t}{X_L}$ .

The ideal heat transfer coefficient is then corrected using the product of five correction factors to provide the shell-side heat transfer coefficient  $h_s$ :

$$h_s = J_c J_L J_B J_S J_R h_{id} \quad (2)$$

The numerical values of the correction factors were determined by Bell and with a subsequent curve-fitting procedure due to [4].

$J_c$  is the correction factor for the baffle cut and spacing and is the average for the entire exchanger. It is expressed as a fraction of the number of tubes in cross flow:

$$J_c = 0.55 + 0.72 F_c \quad (3)$$

Where:

$$F_c = \frac{1}{\pi} [\pi + \varphi \sin(\arccos \varphi) - 2 \arccos \varphi] \quad \text{and} \quad \varphi = \frac{D_s - 2l_c}{D_o}$$

In these equations  $D_s$  is the shell inside diameter (m),  $D_o$  is the diameter at the outer tube limit (m) and  $l_c$  is the distance from the baffle tip to the shell inside diameter (m).

$J_L$  is the correction factor for baffle leakage effects, including both the tube-to baffle and the baffle-to-shell effects (the A and E streams in Fig. 1):

$$J_L = 0.44(1 - r_a) + [1 - 0.044(1 - r_a)] e^{-2.2 r_b} \quad (4)$$

Where

$$r_b = \frac{A_{sb} + A_{tb}}{A_w} \quad \text{and} \quad r_a = \frac{A_{sb}}{A_{sb} + A_{tb}}$$

$J_B$  is the correction factor for bundle and partition bypass effects (the C and F streams in Fig. 1):

$$J_B = \begin{cases} 1 & \text{for } \zeta \geq \frac{1}{2} \\ e^{-C \left[ 1 + 2\zeta^4 \right]} & \text{for } \zeta < \frac{1}{2} \end{cases} \quad (5)$$

Where:

$$r_c = \frac{A_{bp}}{A_w}, \quad \zeta = \frac{N_{ss}}{N_{cc}}$$

Where with  $X_L$  as the longitudinal tube pitch and  $N_{ss}$  taken as the number of sealing strip pairs,

$$N_{cc} = \frac{D_s - 2l_c}{X_L}, \quad C = \begin{cases} 1.35 & \text{for } Re \leq 100 \\ 1.25 & \text{for } Re > 100 \end{cases}, \quad A_{bp} = L_{bc} (D_s - D_o + 0.5 N_p W_p)$$

is the cross flow area for the bypass, where  $N_p$  is the number of bypass divider lanes that are parallel to the crossflow stream B,  $w_p$  is the width of the bypass divider lane (m) and  $L_{bc}$  is the central baffle spacing.

$J_s$  is the correction factor that accounts for variations in baffle spacing at the inlet and outlet sections as compared to the central baffle spacing:

$$J_s = \frac{N_b - 1 + (L_i^*)^{1-n} - (L_o^*)^{1-n}}{N_b - 1 + (L_i^*)^{1-n} + (L_o^*)^{1-n}} \quad (6)$$

Where  $N_b$  is the number of baffles and

$$L_o^* = \frac{L_{bo}}{L_{bc}}, \quad L_i^* = \frac{L_{bi}}{L_{bc}}, \quad n = \begin{cases} \frac{3}{5} & \text{for turbulent flow} \\ \frac{1}{3} & \text{for laminar flow} \end{cases}$$

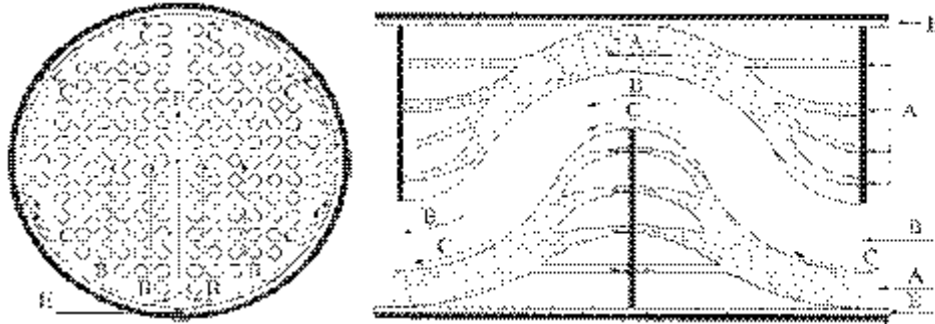


Fig. 1: Tinker model for the shell-side flow streams

Here  $L_{bi}$  is the baffle spacing at the inlet (m),  $L_{bo}$  is the baffle spacing at the outlet (m) and  $L_{bc}$  is the central baffle spacing (m)

$J_R$  is the correction factor that accounts for the temperature gradient when the shell-side fluid is in laminar flow:

$$J_R = \begin{cases} 1 & \text{for } Re_s \geq 100 \\ \left(\frac{10}{N_{r,c}}\right)^{0.18} & \text{for } Re_s \leq 20 \end{cases} \quad (7)$$

For  $20 < Re_s < 100$ , a linear interpolation should be performed between the two extreme values. In equation (7),  $Re_s$  is the shell-side Reynolds number and  $N_{r,c}$  is the number of effective tube rows crossed through one crossflow section.

### CALCULATION OF SHELL SIDE PRESSURE DROP

Tinker suggested a flow stream model for the determination of shell-side pressure loss. Willis and Johnston developed a simpler method which extends Tinker's scheme to include end-space pressure losses and includes a simple method for nozzle pressure drop developed by Grant.

The flow streams in the Willis and Johnston method [16] are shown in Fig. 2. For each of the streams, a coefficient  $n$  is defined so that:

$$n_i = \frac{\Delta P_i}{\dot{m}_i} \quad (i=b, c, s, t, w) \quad (8)$$

where the  $\Delta P_i$ 's and the  $\dot{m}_i$ 's are the pressure drops and mass flow rates for the  $i$ th stream, respectively. The crossflow stream contains the actual crossflow path (path c) and the bypass path (path b). These paths merge into the window stream (path w) and continuity and compatibility for these three paths give

$$\dot{m}_{cr} = \dot{m}_w \quad (9)$$

Where:  $\dot{m}_{cr} = \dot{m}_b + \dot{m}_c$

And the pressure loss between points A and B will be

$$\dot{m}_{cr} = \dot{m}_b + \dot{m}_c, \Delta P_{AB} = \Delta P_{cr} + \Delta P_w, \Delta P_{cr} = \left[ \left(\frac{1}{n_b}\right)^2 + \left(\frac{1}{n_c}\right)^2 \right] \dot{m}_w^2 \quad (10)$$

For the parallel combination of the shell-to-baffle leakage path (path s) and the tube-to-baffle leakage path (path t),

$$\Delta P_l = \left[ \left(\frac{1}{n_s}\right)^2 + \left(\frac{1}{n_t}\right)^2 \right] \dot{m}_l^2 \quad (11)$$

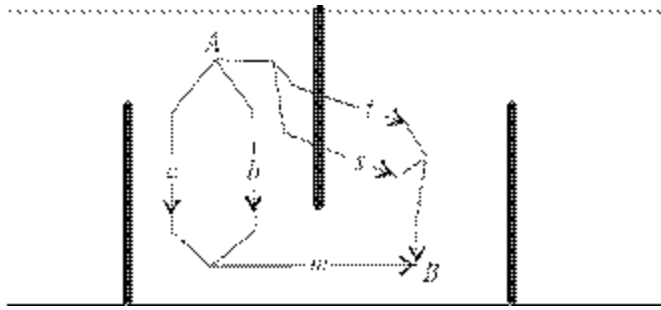


Fig. 2: Shell-side flow streams for the Willis and Johnston pressure-drop method

Where: the leakage flow rate is:  $\dot{m}_l = \dot{m}_s + \dot{m}_t$

A simple computation then determines the total baffle-space pressure loss via

$$\Delta p_{AB} = \Delta P_{cr} + \Delta P_w \tag{12}$$

Where  $\Delta P_{cr} = n_c \dot{m}_c$  or  $\Delta P_{cr} = n_b \dot{m}_b$ ,  $\Delta P_w = n_w \dot{m}_w$

The total pressure loss contains components due to the baffle-space pressure loss established by the foregoing procedure, the end-space pressure loss and the nozzle pressure loss. The end-space pressure loss is taken as

$$\Delta P_e = N_e \dot{m}_e^2 + \frac{1}{2} n_{we} \dot{m}_w^2 \tag{13}$$

Where

$$n_e = n_{cr} + \frac{D_s + \delta_0 v}{2\delta_0 v} \left( \frac{l_{bc}}{l_{be}} \right)^2$$

with

$$n_{cr} = \left[ \left( \frac{1}{n_t} \right)^{1/2} + \left( \frac{1}{n_c} \right)^{1/2} \right]^{-2}$$

And where:

$$n_{we} = \frac{1.9 \text{Exp} \left( 0.6856 \left( \frac{A_w l_{bc}}{A_{cl} l} \right) \right)}{2\rho A_w^2} \tag{14}$$

Grant gives the pressure drop in the inlet nozzle as

$$\Delta P_{ni} = \frac{G_1^2 A_1}{\rho_1 A_2} \left( \frac{A_1}{A_2} - 1 \right) \tag{15}$$

where  $G_1$  is the entry mass velocity,  $G_1 = \rho_1 u_1$ ,  $A_1$  is the inlet nozzle area and  $A_2$  is the bundle entry area. For the outlet-nozzle pressure loss,

$$\Delta P_{n2} = \frac{G_2^2}{2\rho_2} \left[ 1 - \left( \frac{A_3}{A_4} \right)^2 + \left( \frac{1}{C} - 1 \right)^2 \right] \tag{16}$$

Where  $G_2$  is the exit mass velocity,  $G_2 = \rho_2 u_2$ ,  $A_3$  is the outlet nozzle area and  $A_4$  is the bundle exit area. The recommended value of the contraction coefficient is  $C = 2/3$ .

The total shell-side pressure loss will be

$$\Delta P_t = \Delta P_{ni} + (F_T + 1) \Delta P_e + (N_b - 1) \Delta P_{AB} \Delta P_{n2}$$

Above equation has assumed that the pressure losses in the end spaces at inlet and outlet are identical. The factor  $F_T$  is the transitional correction factor and is based on the cross flow Reynolds number

$$Re = \frac{\dot{m}_c d_o}{\mu A_c}$$

Where for  $Re_c < 300$ , the entire method is not valid;  $0 = Re_c < 1000$ ,  $F_T = 3.646e^{-0.1934}$ ; and  $Re_c = 1000$ ,  $F_T = 1$ .

## RESULTS AND DISCUSSION

In this paper, the effect of baffle spacing for STHXs (42E-13014) Iran, Arvand Petrochemical with geometric parameters and thermo-physical properties (Table 1 and 2), is considered. A program in EES (Engineering Equations Solver) software is used for this purpose to solve governing equations and Aspen B-JAC and HTFS<sup>+</sup> software is used for considering estimated total price. The computations are carried out using optimal flow chart Babu and Munawar [17]. For this purpose, according to technical specifications and input fluids conditions the program was run for that STHX has 16 baffles (initial baffle spacing is 9.6 inches). In this case output temperatures from this program are 2.5 percent less than experimental temperatures and output pressure from this program are 4 percent more than experimental pressure. To reconfirm the accuracy of the program, the number of baffles became 12 and again output temperature and pressure from the program were compared to experimental data. In this new case, output temperatures from this program are 2.5 percent less than experimental temperatures and output pressure from this program are 4 percent more than experimental pressure.

After validation of numerical model, the effect of baffle spacing variations from 4 to 24 inches (from 9 to 52 baffles) was considered on heat transfer, pressure drop and estimated total price. It is necessary to say that according to TEMA standard [6] “Segmental baffles normally should not be spaced closer than 1/5 of the shell inside diameter or 2 inches, whichever is greater” and shell inside diameter, the least baffle spacing is considered 4 inches. From this study we conclude that:

1. Required tube length for a given heat duty decreases due to decrease of baffle spacing, so the number of baffles will increase (Fig. 3). When the baffle spacing is 4 inches, the number of baffles is 52 and when the baffle spacing is 24 inches, the number of baffles is 9.
2. Variation of shell side pressure drop versus baffle spacing is shown in Fig. 4. It is found that with the increase of baffle spacing, pressure drop decreases, but after increasing baffles more than 12 inches, variation in pressure drop is gradual and approximately constant. When the baffle spacing decrease from 9.6 (initial baffle spacing) to 4 inches, corresponding number of baffles increase from 16 to 52. And when baffle spacing is 4 inches, shell side pressure drop is about 6 times as much as initial baffle spacing.
3. Figure 5 and 6 Show that variation of shell side convection heat transfer coefficient (film coefficient) versus baffle spacing and overall heat transfer coefficient (OHTC) versus baffle spacing. It can be found that shell side

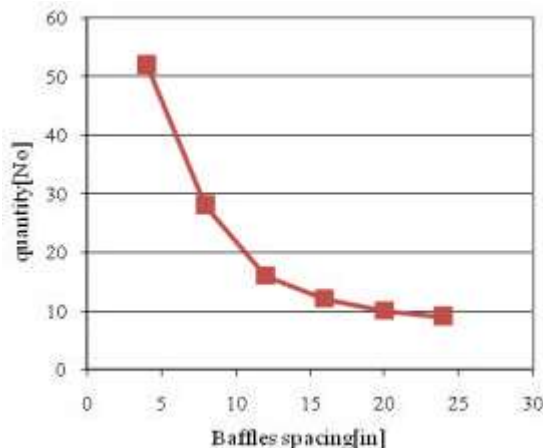


Fig. 3: Baffles quantity versus baffle spacing

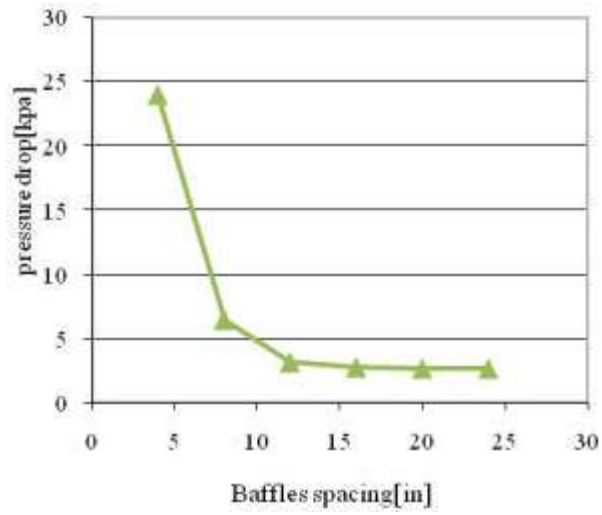


Fig. 4: Shell side Pressure drop versus baffle spacing

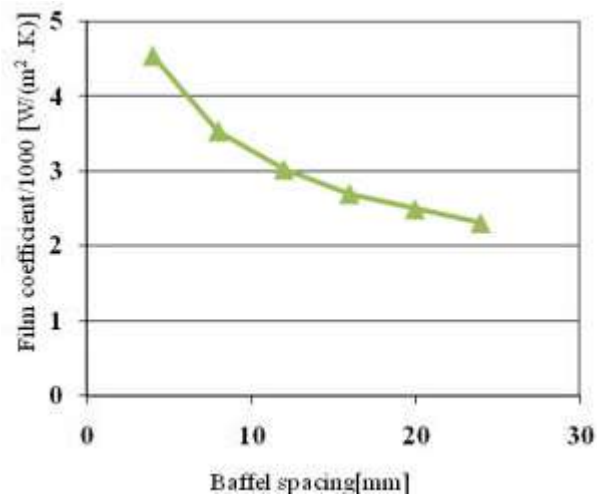


Fig. 5: Shell side convection heat transfer coefficient versus baffle spacing

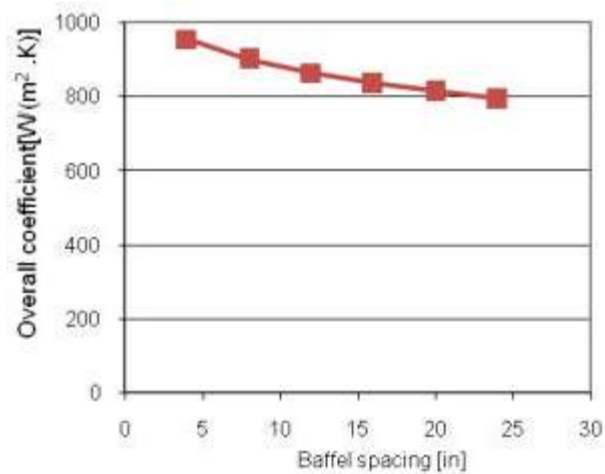


Fig. 6: Overall heat transfer coefficient versus baffle spacing

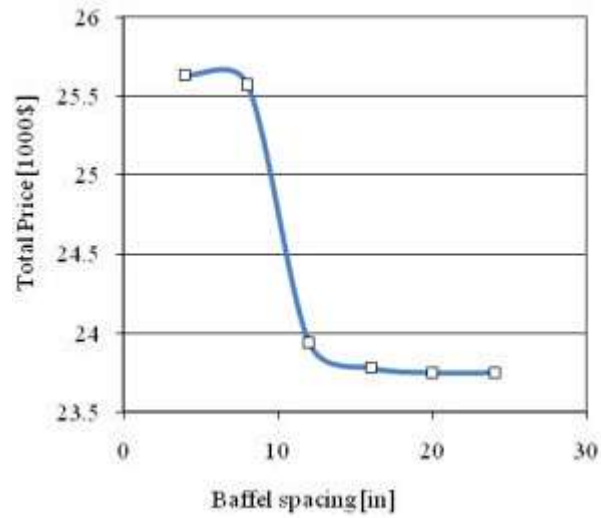


Fig. 7: Estimated total price versus baffle spacing

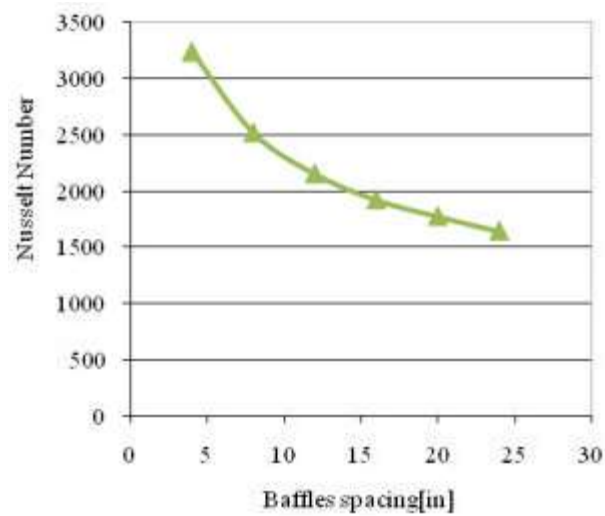


Fig. 8: Average Nusselt number over tubes versus baffle spacing

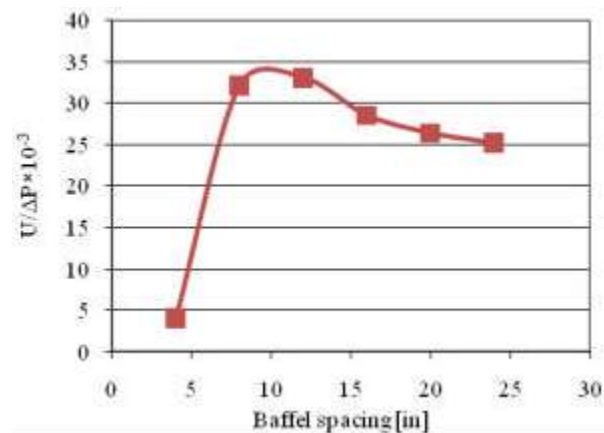


Fig. 9: Overall heat transfer coefficient to pressure drop ratio versus baffle spacing



convection heat transfer coefficient and OHTC have inverse relationship with baffle spacing. If baffle spacing decreases from 9.6 to 4 inches, shell side convection heat transfer coefficient will increase 1.5 times as much as initial baffle spacing. Also when baffle spacing is 24 inches, OHTC is about 24 percent lower than when baffle spacing is 4 inches.

4. Variation of estimated total price versus baffle spacing is shown in Fig. 7. It is necessary to say that in this Figure total price is estimated by Aspen B-Jac and HTFS<sup>+</sup> softwares. If baffle spacing increases OHTC will decrease (Fig. 6), so the required heat transfer surface must be increased to reach to operation temperature. As a result variation of baffle spacing has a direct influence on total price. As Fig. 7 shows STHX with baffle spacing between 10 to 20 inches has minimum total price and STHX with 4 inches baffle spacing has maximum temperature.
5. Figure 8 shows Average Nusselt number over tubes versus baffle spacing. It can be observed in Fig. 8. That Nusselt number has inverse relationship with baffle spacing. The decrease of baffle spacing causes the increase of Nusselt number over tubes, so OHTC increases. The decrease of baffle spacing from initial spacing (9.6 inches) to 4 inches causes the increase of Nusselt number about 1.5 times. Moreover, the decrease of baffle spacing from 24 inches to 4 inches causes the increase of Nusselt number about 2 times and OHTC increases 24 percent.
6. Overall heat transfer coefficient to pressure drop ratio ( $U/\Delta p$  ratio) versus baffle spacing is shown in Fig. 9. According to Fig. 9  $U/\Delta p$  ratio is the least when baffle spacing is 4 inches because pressure drop is maximum. Then with increase of baffle spacing,  $U/\Delta p$  ratio increases because pressure drop rapidly decreases (Fig. 4), but the decrease of OHTC is lower than the decrease of pressure drop. After increasing baffles more than 12 inches, variation in pressure drop is gradual and approximately constant and OHTC decreases; Consequently,  $U/\Delta p$  ratio decreases again.

## CONCLUSIONS

Comparison of variation of OHTC, shell side pressure drop and estimate total price in a STHX according to baffle spacing (Fig. 4-7) shows that when baffle spacing is 4 inches, pressure drop and OHTC are both maximum, but in this case pressure drop is about 6 times as much as initial baffle spacing and estimated total price increases 7 percent. This is not suitable because initial cost increases and current cost increases desperately because of very high pressure drop. After increasing baffles more than 12 inches, variation in pressure drop is gradual and approximately constant and OHTC decreases; Consequently,  $U/\Delta p$  ratio decreases again. If baffle spacing reaches to 24 inches, STHX will have minimum pressure drop, but OHTC decreases, so required heat transfer surface increases and  $U/\Delta p$  ratio decreases. So optimum baffle spacing is suggested between 8 to 12 inches (43 to 63 percent of inside shell diameter) for a sufficient heat duty, low cost and low pressure drop.

## ACKNOWLEDGEMENT

This work is based on a research proposal founded by Islamic Azad University.

## REFERENCES

1. Nasiruddin, M.H. and K. Siddiqui, 2007. Heat transfer augmentation in a heat exchanger tube using a baffle. *International Journal of Heat and Fluid Flow*, 28 (2): 318-328
2. Bell, K.J., 1988. Delaware Method for Shell Side Design. In *Heat Transfer Equipment Design*. Shah, R.K., E.C. Subbarao and R.A. Mashelkar (Eds.). Hemisphere Publishing, New York, pp: 145-166.
3. Bejan, A. and A.D. Kraus, 2003. *Heat Transfer Hand Book*. New York: Wiley.
4. Taborek, J., 1998. Shell-and-Tube Heat Exchangers in Single Phase Flow. In *Handbook of Heat Exchanger Design*. Begell House, New York.
5. Taborek, J., 1983. Shell-and-Tube Heat Exchangers. In *Heat Exchanger Design Handbook*. E.U. Schlunder (Ed.). Hemisphere Publishing, New York.
6. Richard, C., 2007. Standards of Tubular Exchanger Manufacturers Association (TEMA). Nine Edition, Byrne, Secretary, New York.

7. Shah, R.K. and D. Sekulic, 2003. Fundamentals of Heat Exchanger Design. Wiley New York.
8. Iqbal, M.J., N.A. Sheikh, H.M. Ali, S. Khushnood and M. Arif, 2012. Comparison of empirical correlations for the estimation of conjugate heat transfer in a thrust chamber. *Life Sci. J.*, 9 (4): 708-716.
9. Hafshejani, M.K., F. Khandani, R. Heidarpour, A. Sedighpour, H. Fuladvand, R. Shokuhifard and A. Arad, 2012. Study of the health threatening mercury effective parameters for its removal from the aqueous solutions by using activated carbons. *Life Sci. J.*, 9 (4): 1789-1791.
10. Aboalizadeh, Z., Y. Arabnia, S. Tabrizi and A. Taherkhani, 2012. A comparison between Curie temperature of nano and bulk Al doped nickel ferrite (NiAlFeO<sub>4</sub>). *Life Sci. J.*, 9 (3): 1221-1225.
11. Hong, B., W. Wang, X. Wang, J. Wang and M. Ye, 2012. Numerical Simulation to Get Flow Pattern in Modified Carotid Artery Bifurcation Model Using PIV. *Life Sci. J.*, 9 (3): 1296-1301.
12. Tong, T.O. and M.T. Kambule, 2012. Total stress tensors and heat fluxes of single flow through a porous viscoelastic medium. *Life Science Journal*, 9 (1): 1-12.
13. Huadong, L. and K. Volker, 1998. Effect of baffle spacing on pressure drop and local heat transfer in shell-and-tube heat exchangers for staggered tube arrangement. *International Journal: Heat and Mass & Transfer*, 41 (10): 1303-1311.
14. Fraas, A.P., 1989. Heat Exchanger Design. Wiley, New York.
15. Zhukauskas, A.A., 1987. Convective Heat Transfer in Cross Flow. In: *Handbook of Single-Phase Convective Heat Transfer*. Kakac, S., R.K. Shah and W. Aung, (Eds.). Wiley, New York.
16. Willis, M.J.N. and D. Johnston, 1984. A New and Accurate Hand Calculation Method for Shell Side Pressure Drop and Flow Distribution. ASME-HTD-36, New York, pp: 67-79.
17. Babu, B.V. and S.A. Munawar, 2007. Differential evolution strategies for optimal design of shell-and-tube heat exchangers. *Chemical Engineering Science*, 62 (2): 3720-3739.